

# Nonequilibrium Spectroscopy of Topological Edge Liquids

Stanislav S. Apostolov and Alex Levchenko

*Department of Physics and Astronomy, Michigan State University, East Lansing, Michigan 48824, USA*

(Dated: May 19, 2014)

We develop a theory for energy and spatially resolved tunneling spectroscopy of topological quantum spin Hall helical states driven out of equilibrium. When a helical liquid is constrained between two superconducting reservoirs transport at the edge is governed by multiple Andreev reflections. The resulting quasiparticle distribution functions of the edge channels exhibit multiple discontinuities at subgap energies with the periodicity of an applied voltage. The combined effect of interactions, disorder, and normal scattering off the superconducting interface leads to the inelastic processes mixing different helicity modes, thus causing smearing of these singularities. If equilibration is strong, then the distribution functions of the edge channels tend to collapse into a Fermi-like function with an effective temperature determined by the superconducting gap, applied voltage, and intraedge interaction parameter. We conclude that mapping out nonequilibrium distribution functions may help to quantify the relative importance of various relevant perturbations that spoil ideally ballistic edge transport.

PACS numbers: 71.10.Pm, 72.10.-d, 74.45.+c

Energy and spatially resolved tunneling experiments provide extremely sensitive spectroscopic tools for accessing and characterizing nonequilibrium states. This technique was introduced in the context of mesoscopic quantum wires [1–3] and later successfully applied to probe quasiparticle distributions in carbon nanotubes [4] and the edge channels of the integer quantum Hall effect [5]. The power of such experiments is that they allow one to deduce the scaling of quasiparticle lifetimes on energy and also to elucidate the microscopic scattering processes responsible for the relaxation. Motivated by these experimental capabilities, we develop a theory for the out-of-equilibrium energy-resolved spectroscopy of a new class of one-dimensional liquids as realized in the quantum spin Hall (QSH) insulators [6, 7].

A key signature of the QSH effect is the appearance of gapless edge states coexisting with gapped bulk states. These edge modes counterpropagate and carry opposite spins. Such correlation between the direction of motion and spin orientation facilitates the term helical liquid [8]. Owing to protection by time-reversal symmetry, helical modes are immune to single-particle elastic backscattering by nonmagnetic disorder, thereby providing opportunities for dissipationless transport with a universally quantized temperature-independent conductance of  $e^2/h$  per helical edge. This expectation has been confirmed experimentally in the topologically nontrivial phase of HgTe/HgCdTe and InAs/GaSb heterostructures hosting helical edge states with observed conductance close to the quantum value [9, 10]. However, clear deviations from this limit have also been identified: the conductance is suppressed for increasing system size [11–15], thus implying the presence of inelastic relaxation. These findings have attracted a great deal of theoretical attention and triggered multiple proposals for possible scattering mechanisms affecting the ideally ballistic edge transport [6, 8, 16–25]. We briefly summarize various scenarios

for the equilibration processes and temperature scaling of the corresponding scattering rates.

The most obvious reason for electron backscattering is magnetic disorder that can flip the spin and thus induce transitions between counterpropagating edge modes. The rate of this process follows a power-law temperature dependence  $T^{2K-2}$  at low temperatures with the exponent determined by the Luttinger liquid interaction parameter  $K$  [8, 17, 19, 25]. The same temperature scaling of the current backscattered from an impurity applies to the case when time-reversal symmetry is broken directly by an applied magnetic field. If time-reversal symmetry is preserved then the leading-order inelastic processes involve backscattering of electron pairs [6, 8, 16, 21, 22, 25]. The latter are either umklapp or disorder-mediated processes due to momentum nonconservation. Umklapp scattering has an exponentially slow rate  $e^{-E_F/T}$  unless the Fermi energy  $E_F$  is tuned to the immediate vicinity of the Dirac point. Impurity-assisted scattering is less susceptible to the position of the Fermi level, and the corresponding rate scales as  $T^{4K}$  or  $T^{8K-2}$  depending on whether  $K \gtrless 1/2$ . The above arguments apply to helical liquids that possess an additional axial symmetry. It has been recently emphasized [18, 20, 26, 27] that such an auxiliary symmetry, if present in the system, could be easily lifted by the combined effect of a strong spin-orbit interaction and backgate-induced electric field which causes the spin quantization axis to rotate with the momentum. This mechanism opens a new channel for inelastic scattering, namely single-particle backscattering accompanied by particle-hole excitation, which also requires impurities to remove constraints imposed by momentum conservation. The rate of this process scales with energy as  $T^{2K+2}$ . Interestingly, the same mechanism also allows single-particle backscattering even for the translationally invariant edge, however with a slower rate due to kinematic constraints.

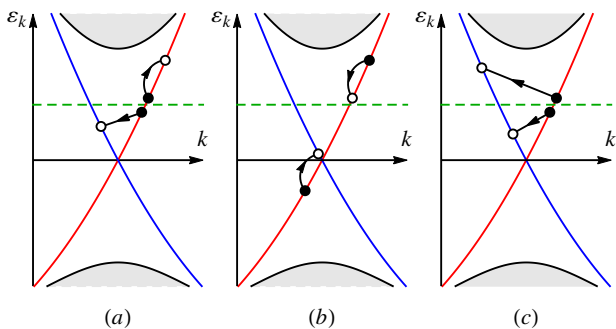


FIG. 1: An allowed backscattering processes: (a) single-particle backscattering accompanied by particle-hole excitation. At weak interactions  $K \simeq 1$  the rate of this process scales with temperature as  $T^4$ . (b) Umklapp scattering, which goes with a rate  $\propto T^5$  if the Fermi energy is tuned to the time-reversal invariant point  $T \gg E_F$ , while this rate is exponentially suppressed as  $\propto e^{-E_F/T}$  in the opposite limit  $T \ll E_F$ . (c) Impurity-assisted inelastic two-particle backscattering that scales with the temperature as  $T^6$ .

Figure 1 summarizes the leading inelastic two-particle processes for the time-reversal-symmetric QSH edge.

The value of the Luttinger liquid interaction parameter  $K$  within the edge states depends on the details of the heterostructure and materials. It can be estimated as  $K = [1 + r_s \ln(d/a)]^{-1/2}$ , where  $r_s = 2e^2/\pi^2 v_F \kappa$  is the electron gas parameter,  $d$  is the distance to a nearby metallic gate, and  $a$  is the short-distance cutoff for the Coulomb interaction, which is either determined by the microscopic screening length or the thickness of the quantum well. For typical values of the Fermi velocity  $v_F \simeq 5 \times 10^5$  m/s and high dielectric constant  $\kappa \simeq 12$  of HgTe, one estimates  $K > 0.9$  for values of  $\ln(d/a) < 3$ . In the following we concentrate on the weakly interacting limit assuming  $K \simeq 1$ .

Given the plethora of scattering events, it is desirable to have an experimental probe that may potentially distinguish between different possibilities or perhaps elucidate their relative importance. As alluded to at the beginning, such a probe may be provided by energy-resolved spectroscopy of the helical edge channels, and our motivation is to develop corresponding theory. We propose to consider a QSH edge that is constrained between two ordinary  $s$ -wave superconductors and driven out of equilibrium by an applied voltage  $V$  between them. We assume that due to the proximity effect the superconductors induce a gap  $\Delta$  over a finite length  $l$  of the helical liquid. The latter is determined by the lithographic thickness of the superconducting leads, which we assume to be up to a few times larger than the superconducting coherence length  $l \gtrsim \xi = v_F/\Delta$ . The distance  $L$  between the superconductors is assumed to be in the limit  $L \gg \{l, \xi\}$ . We are interested in calculating the energy and spatially dependent profiles of the distribution functions  $f_\varepsilon^\pm(x)$  for

the right- and left-moving ( $\pm$ ) helicity channels, neither of which is assumed to be approximated by the equilibrium Fermi function. We demonstrate that  $f_\varepsilon^\pm(x)$  is extremely sensitive to the interaction effects and relevant perturbations affecting ideally ballistic transport. The choice in favor of the above specified geometry is twofold. First, at small voltages  $eV < \Delta$  the transport along the edge is governed by multiple Andreev reflections (MAR), which strongly magnify the structure of the distribution functions  $f_\varepsilon^\pm(x)$  at subgap energies, thus making it easily detectable experimentally. Second, due to MAR trajectories quasiparticles traverse the edge between superconductors many times, which effectively increases the probability of inelastic scattering even for relatively weak interactions. It should be stressed that MAR have been recently observed in the QSH regime of InAs/GaSb quantum wells [28] and in InSb/InAs nanowires [29]. Induced superconductivity has also been achieved in QSH channels of HgTe/HgCdTe heterostructures [30]. Our focus on inelastic scattering complements other recent interesting proposals addressing nonequilibrium transport and proximity-effect-related phenomena with QSH edges [27, 31–36]. Furthermore, our work may also be of special interest in view of ongoing efforts in studying equilibration of one-dimensional liquids beyond the Luttinger liquid paradigm where inelastic multiparticle scattering processes play a central role [37–42].

The method of calculating the distribution functions that we employ in this study is based on the quantum kinetic equation

$$\pm \partial_x f_\varepsilon^\pm(x) = -\text{St}\{f_\varepsilon^\pm(x)\}. \quad (1)$$

The same technique has been previously used to describe ballistic and diffusive superconductor–normal-metal wire–superconductor (SNS) quasi-one-dimensional proximity circuits in the regime of MAR [43, 44]. The collision integral  $\text{St}\{f_\varepsilon^\pm\}$  of the kinetic equation (1) depends on a particular type of scattering affecting the distribution function. Although all the backscattering processes shown in Fig. 1 appear to be of the same order in interaction (at least in the weak-coupling limit), we choose inelastic single-particle backscattering [Fig. 1(a)] as a guiding example. The reason for this is based on the observation that this process has the lowest scaling with energy, which implies the fastest relaxation time. Furthermore, this scattering does not assume axial spin symmetry, which is expected to be a generic feature of helical states. The corresponding collision integral reads

$$\begin{aligned} \text{St}\{f_\varepsilon^\alpha\} = & -\lambda \sum_{\beta\sigma\varsigma=-\alpha} \iint d\varepsilon_1 d\varepsilon_2 M_{\varepsilon,\varepsilon_1,\varepsilon_2}^{\alpha\beta} \\ & [f_\varepsilon^\alpha f_{\varepsilon_1-\varepsilon_2}^\beta g_{\varepsilon-\varepsilon_2}^\sigma g_{\varepsilon_1}^\varsigma - g_\varepsilon^\alpha g_{\varepsilon_1-\varepsilon_2}^\beta f_{\varepsilon-\varepsilon_2}^\sigma f_{\varepsilon_1}^\varsigma], \end{aligned} \quad (2)$$

where summation over the helicity indices  $\beta, \sigma$  and  $\varsigma$  goes in such a way that their product equals  $-\alpha$ . The

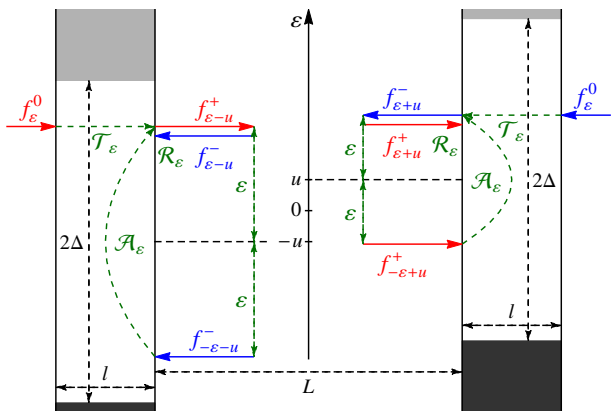


FIG. 2: The scheme of energy bands for multiple Andreev reflection trajectories. Horizontal dashed lines at  $\pm u$  represent Fermi levels of superconductors,  $u = eV/2\Delta$ . Lines with arrows represent incoming and outgoing particles reflected via normal or Andreev processes with corresponding coefficients and occupation factors indicated on the diagram.

kernel of the collision integral is quadratic in energy  $M_{\varepsilon, \varepsilon_1, \varepsilon_2}^{\alpha\beta} = (\varepsilon - \varepsilon_1 + \alpha\beta\varepsilon_2)^2$ , and we also introduced the notation  $g_{\varepsilon}^{\pm} = 1 - f_{\varepsilon}^{\pm}$ . In Eq. (1) we rescaled the coordinate  $x \rightarrow x/L$ , while in Eq. (2) we rescaled all energies in units of the superconducting gap,  $\varepsilon \rightarrow \varepsilon/\Delta$ , so that the interaction parameter  $\lambda$  is explicitly dimensionless. Its precise value depends on the model. For example, for the case of sharp disorder it can be derived perturbatively to second order in electron-electron and electron-impurity scattering with the result  $\lambda \simeq [(U_0 + U_{2k_F})W_{2k_F}/4v_F^2]^2(\Delta/k_0v_F)^4$ , where  $U_0, U_{2k_F}$ , and  $W_{2k_F}$  are the Fourier components of the Coulomb and impurity potentials, respectively, while  $k_0$  parametrizes the scale on which the spin quantization axis rotates with momentum [20]. In our analysis we keep  $\lambda$  as a small adjustable parameter. It is worth noting that the same collision integral as in Eq. (2) appears in a different model of disorder [24], namely, spontaneously formed quantum dots representing the large-scale inhomogeneities of electron and hole puddles.

The kinetic equation should be supplemented by appropriate boundary conditions connecting  $f_{\varepsilon}^{\pm}$  to the distribution functions in the reservoirs  $f_{\varepsilon}^0$ , which are simply the Fermi functions. This can be accomplished by the following relations at the interfaces

$$f_{\varepsilon \pm u}^{\mp} = \mathcal{A}_{\varepsilon}(1 - f_{-\varepsilon \pm u}^{\pm}) + \mathcal{R}_{\varepsilon}f_{\varepsilon \pm u}^{\pm} + \mathcal{T}_{\varepsilon}f_{\varepsilon}^0, \quad x = \pm 1/2, \quad (3)$$

with  $u = eV/2\Delta$ . For technical convenience in further numerical calculations, we choose to measure the excitation energy with respect to a point halfway between the electrochemical potentials in the superconductors. The corresponding energy diagram connected to the boundary conditions (3) and MAR trajectories is shown in Fig. 2. The first term on the right-hand side of Eq. (3) corresponds to the Andreev process which is based on

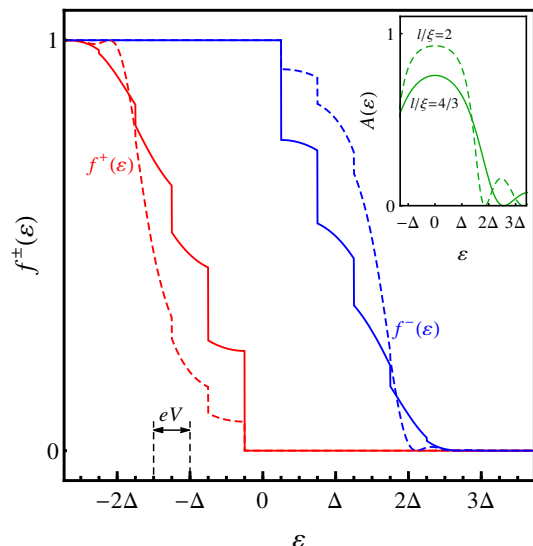


FIG. 3: Nonequilibrium distribution functions  $f_{\varepsilon}^{\pm}$  in the absence of inelastic scattering for  $l/\xi = 4/3$  (solid line) and  $l/\xi = 2$  (dashed line) and  $eV = \Delta/2$ . The inset represents energy dependence of the Andreev reflection coefficient from Eq. (4) for the same choice of ratios  $l/\xi$ .

the fact that  $1 - f^{\pm}$  accounts for the occupation probability that an incident hole with energy  $-\varepsilon$  will reflect with amplitude probability  $\mathcal{A}_{\varepsilon}$  and emerge as an electron with energy  $\varepsilon$ . The other two terms correspond to normal reflection and transmission with respective probabilities  $\mathcal{R}_{\varepsilon}$  and  $\mathcal{T}_{\varepsilon}$ . It is also expected that for energies deep below the superconducting gap  $\varepsilon \ll -1$ , the distribution functions saturate to unity  $f_{\varepsilon}^{\pm} \rightarrow 1$  since such states are fully occupied, whereas  $f_{\varepsilon}^{\pm} \rightarrow 0$  in the opposite case  $\varepsilon \gg 1$  for the highly excited states which are empty (recall that  $\Delta \rightarrow 1$  in the rescaled energy units).

The coefficient of Andreev reflection can be found by solving the auxiliary problem of one-dimensional Dirac fermions impinging on the potential step created by a superconducting strip of width  $l$  with the result

$$\mathcal{A}_{\varepsilon} = \frac{1}{\varkappa_{\varepsilon}^2 \coth^2(l\varkappa_{\varepsilon}/\xi) + \varepsilon^2}, \quad (4)$$

where  $\varkappa_{\varepsilon} = \sqrt{1 - \varepsilon^2}$ . For energies outside of the gap  $\varkappa_{\varepsilon}$  becomes imaginary and  $\mathcal{A}_{\varepsilon}$  undergoes oscillatory decay. One should notice here that for subgap energies and a wide superconductor,  $l \gg \xi$ , the Andreev coefficient  $\mathcal{A}_{\varepsilon}$  is nearly unity. For a narrower superconductor with  $l \sim \xi$  the evanescent Bogoliubov quasiparticle wave survives and thus reduces  $\mathcal{A}_{\varepsilon}$  in absolute value. This behavior is illustrated in the inset of Fig. 3.

For ideal edge channels with an additional spin axial symmetry the normal reflection coefficient  $\mathcal{R}_{\varepsilon}$  is identically zero. Indeed, in the course of normal reflection an electron changes its direction of propagation but conserves its spin, which is not possible due to the helicity

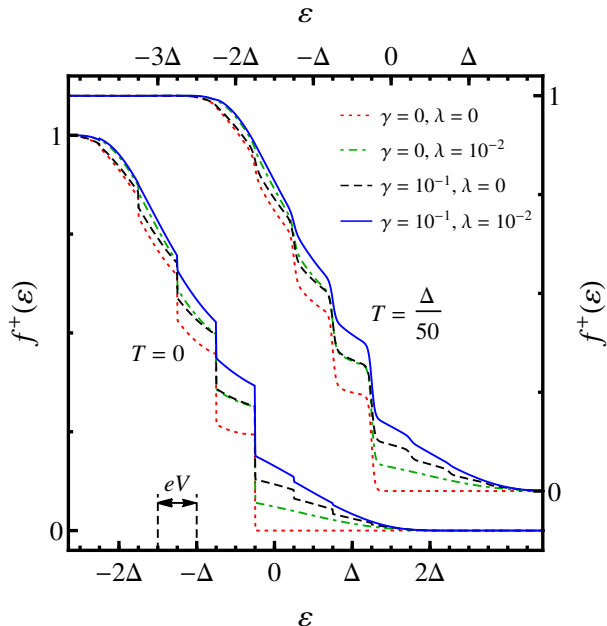


FIG. 4: Nonequilibrium distribution functions  $f_{\varepsilon}^{\pm}$  plotted for the case  $l/\xi = 4/3$  and  $eV = \Delta/2$  at different values of parameters  $\gamma$  and  $\lambda$  quantifying normal and inelastic scattering, and also at different temperatures  $T = 0$  and  $T = \Delta/50$ .

constraint in an ideal QSH edge state. However, for a generic helical liquid one expects to have a finite probability of normal reflection. Calculation of the energy dependence of  $\mathcal{R}_{\varepsilon}$  is a difficult task since the result depends on the actual mechanism that lifts spin symmetry and also on the details of the heterostructure. We suspect that the precise energy dependence of  $\mathcal{R}_{\varepsilon}$  is not of principal importance because this coefficient is small and can be treated as a perturbation. We take in our modeling  $\mathcal{R}_{\varepsilon} = \gamma \mathcal{A}_{\varepsilon}$  with  $\gamma \ll 1$  being a second control parameter of the theory. In the case of conventional superconductor-normal-metal junctions the parameter  $\gamma$  is small in the ratio of the energy gap to the Fermi energy  $\Delta/E_F \ll 1$ . In the context of the QSH proximity effect the Fermi energy is replaced by the bulk band gap of the material  $E_G$ . Furthermore,  $\gamma$  acquires an additional smallness due to off-diagonal terms in spin space since the spin has to rotate for normal reflection to occur. Based on the  $\mathbf{k} \cdot \mathbf{p}$  calculations of Ref. [26] one may estimate  $\gamma \sim (\mathcal{E}_z/\mathcal{E}_0)(\Delta/E_G)$ , where  $\mathcal{E}_z$  is the electric field generated perpendicular to the plane of a quantum well and  $\mathcal{E}_0 \sim 100\text{mV/nm}$ . For  $E_G \sim 10\text{meV}$  and a conventional superconductor, a conservative numerical estimate for normal reflection gives  $\gamma \lesssim 0.1$ . In the calculations we use  $\mathcal{A}_{\varepsilon}$  from Eq. (4), choose  $\gamma$  as a variable small parameter, and enforce  $\mathcal{T}_{\varepsilon} = 1 - \mathcal{A}_{\varepsilon} - \mathcal{R}_{\varepsilon}$ .

The nonequilibrium distribution functions  $f_{\varepsilon}^{\pm}$  of an ideal QSH edge channel can be found analytically. In the absence of inelastic scattering the collision integral

in Eq. (2) drops out from the kinetic problem and should be replaced by the condition  $f_{\varepsilon}^{\pm}|_{x=-1/2} = f_{\varepsilon}^{\pm}|_{x=1/2}$ . If we rewrite this condition in terms of the energy measured with respect to the local value of the electrochemical potential it takes the form  $f_{\varepsilon}^{\pm}|_{x=-1/2} = f_{\varepsilon-2u}^{\pm}|_{x=1/2}$  merely stating that electrons with energy  $\varepsilon$  at  $x = -1/2$  have different energy when they arrive at the other superconductor at  $x = 1/2$  due to the applied voltage bias along the edge. When combined with the boundary conditions, Eq. (3), one obtains a closed set of recursion relations, which can be resolved in the form

$$f_{\varepsilon}^{\pm} = \sum_{l=0}^{\infty} \left[ \prod_{m=0}^{l-1} \mathcal{A}_{\varepsilon \pm (2m+1)u} \right] \mathcal{T}_{\varepsilon \pm (2l+1)u} f_{\varepsilon \pm (2l+1)u}^0. \quad (5)$$

This result is analogous to ballistic SNS channels [43]. These distributions are plotted in the main panel of Fig. 3 for two different ratios of  $l/\xi$  at zero temperature with thus  $f_{\varepsilon}^0 = \theta_{-\varepsilon}$ , where  $\theta_{\varepsilon}$  is the conventional Heaviside step function. The rich subgap structure of the distribution functions is due to MAR trajectories, and discontinuities appear in steps of the applied voltage. It should be noted, that the case of perfect Andreev reflection,  $\mathcal{A}_{\varepsilon} = 1$ , at zero temperature corresponds to distributions  $f_{\varepsilon}^{\pm}$  that are close to displaced Fermi functions without any special subgap features.

Next we address the role of normal and inelastic scattering on the subharmonic gap structure of the distribution functions. This problem was solved numerically by treating the collision integral in the kinetic equation perturbatively by iterations. We find that a finite value of the normal reflection coefficient leads to an appreciable shift of the discontinuities in the distribution function in their absolute values but not in their positions in energy. Even more importantly, finite value of  $\gamma$  results also in the appearance of new discontinuities at energies near the superconducting gap edges (see Fig. 4). This leads to an interesting conclusion that while the subgap structure of the distribution functions is a consequence of Andreev reflection processes, it is the normal reflection processes which sharpen the structure. Experimentally this feature could be at least a qualitative measure of the normal reflection in QSH devices subject to the proximity effect. The primary role of the inelastic scattering along the edge is to smear subgap discontinuities in the distribution functions and also to extend the tails of these distributions deeper into the regions below and above the superconducting gap. This is qualitatively similar to the finite-temperature effect, which also leads to a substantial broadening of the subharmonic structure as illustrated in Fig. 4. Although the regime of strong equilibration of the helical edges is beyond the scope of this work, we observe that at  $u \ll 1$  increasing the interaction parameter to  $\lambda \sim 1$  is the equivalent of having an effective temperature  $T_{\text{eff}} \sim \Delta/\ln(\lambda/u^2) \ll \Delta$ , and the distribution functions tend to take a Fermi-like shape.

In summary, we have developed a kinetic equation approach for the direct calculation of the distribution functions of the QSH helical edge states. Our model contains the essential physical processes leading to subharmonic gap structure, namely, Andreev and normal reflection processes at superconducting interfaces, as well as inelastic backscattering along the edge. We believe that our theory will be useful for the interpretation of energy-resolved experiments that may help to quantify the degree of intraedge equilibration, and thus strength of interactions and the strength of normal scattering, which is determined by the effects lifting auxiliary spin symmetry of ideal helical edge modes.

- 
- [1] H. Pothier, S. Guéron, N. O. Birge, D. Esteve, and M. H. Devoret, *Phys. Rev. Lett.* **79**, 3490 (1997).
- [2] F. Pierre, A. Anthore, H. Pothier, C. Urbina, and D. Esteve, *Phys. Rev. Lett.* **86**, 1078 (2001).
- [3] A. Anthore, F. Pierre, H. Pothier, and D. Esteve, *Phys. Rev. Lett.* **90**, 076806 (2003).
- [4] Y.-F. Chen, T. Dirks, G. Al-Zoubi, N. O. Birge, and N. Mason, *Phys. Rev. Lett.* **102**, 036804 (2009); N. Bronn and N. Mason, *Phys. Rev. B* **88**, 161409(R) (2013).
- [5] C. Altimiras, H. le Sueur, U. Gennser, A. Cavanna, D. Mailly and F. Pierre, *Nat. Phys.* **6**, 34 (2010); *Phys. Rev. Lett.* **105**, 056803 (2010).
- [6] C. L. Kane and E. J. Mele, *Phys. Rev. Lett.* **95**, 146802 (2005); *ibid* **95**, 226801 (2005).
- [7] B. A. Bernevig and S.-C. Zhang, *Phys. Rev. Lett.* **96**, 106802 (2006).
- [8] C. Wu, B. A. Bernevig, and S.-C. Zhang, *Phys. Rev. Lett.* **96**, 106401 (2006).
- [9] M. König, S. Wiedmann, C. Brüne, A. Roth, H. Buhmann, L. W. Molenkamp, X.-L. Qi, and S.-C. Zhang, *Science* **318**, 766 (2007).
- [10] I. Knez, R.-R. Du, and G. Sullivan, *Phys. Rev. Lett.* **107**, 136603 (2011).
- [11] A. Roth, C. Brune, H. Buhmann, L. W. Molenkamp, J. Maciejko, X.-L. Qi, and S.-C. Zhang, *Science* **325**, 294 (2009).
- [12] G. M. Gusev, Z. D. Kvon, O. A. Shegai, N. N. Mikhailov, S. A. Dvoretzky, and J. C. Portal, *Phys. Rev. B* **84**, 121302(R) (2011).
- [13] M. König, M. Baenninger, A. G. F. Garcia, N. Harjee, B. L. Pruitt, C. Ames, P. Leubner, C. Brüne, H. Buhmann, L. W. Molenkamp, and D. Goldhaber-Gordon, *Phys. Rev. X* **3**, 021003 (2013).
- [14] K. C. Nowack, E. M. Spanton, M. Baenninger, M. König, J. R. Kirtley, B. Kalisky, C. Ames, P. Leubner, C. Brüne, H. Buhmann, L. W. Molenkamp, D. Goldhaber-Gordon, and K. A. Moler, *Nature Materials* **12**, 787 (2013).
- [15] K. Suzuki, Y. Harada, K. Onomitsu, and K. Muraki, *Phys. Rev. B* **87**, 235311 (2013).
- [16] C. Xu and J. E. Moore, *Phys. Rev. B* **73**, 045322 (2006).
- [17] J. Maciejko, C. Liu, Y. Oreg, X.-L. Qi, C. Wu, and S.-C. Zhang, *Phys. Rev. Lett.* **102**, 256803 (2009).
- [18] A. Ström, H. Johannesson, and G. I. Japaridze, *Phys. Rev. Lett.* **104**, 256804 (2010).
- [19] Y. Tanaka, A. Furusaki, and K. A. Matveev, *Phys. Rev. Lett.* **106**, 236402 (2011).
- [20] T. L. Schmidt, S. Rachel, F. von Oppen, and L. I. Glazman, *Phys. Rev. Lett.* **108**, 156402 (2012).
- [21] N. Lezmy, Y. Oreg, and M. Berkooz, *Phys. Rev. B* **85**, 235304 (2012).
- [22] F. Crépin, J. C. Budich, F. Dolcini, P. Recher, and B. Trauzettel, *Phys. Rev. B* **86**, 121106 (2012).
- [23] M. Kharitonov, *Phys. Rev. B* **86**, 165121 (2012).
- [24] J. I. Väyrynen, M. Goldstein, and L. I. Glazman, *Phys. Rev. Lett.* **110**, 216402 (2013).
- [25] E. Eriksson, *Phys. Rev. B* **87**, 235414 (2013).
- [26] D. G. Rothe, R. W. Reinthaler, C.-X. Liu, L. W. Molenkamp, S.-C. Zhang, and E. M. Hankiewicz, *New J. Phys.* **12**, 065012 (2010).
- [27] P. Virtanen and P. Recher, *Phys. Rev. B* **85**, 035310 (2012).
- [28] I. Knez, R.-R. Du, and G. Sullivan, *Phys. Rev. Lett.* **109**, 186603 (2012).
- [29] H. A. Nilsson, P. Samuelsson, P. Caroff, and H. Q. Xu, *Nano Lett.* **12**, 228 (2012).
- [30] S. Hart, H. Ren, T. Wagner, P. Leubner, M. Mühlbauer, C. Brüne, H. Buhmann, L. W. Molenkamp, A. Yacoby, arXiv:1312.2559.
- [31] L. Fu and C. L. Kane, *Phys. Rev. Lett.* **100**, 096407 (2008); *Phys. Rev. B* **79**, 161408 (2009).
- [32] P. Adroguer, C. Grenier, D. Carpentier, J. Cayssol, P. Degiovanni, and E. Orignac, *Phys. Rev. B* **82**, 081303(R) (2010).
- [33] D. M. Badiane, M. Houzet, and J. S. Meyer, *Phys. Rev. Lett.* **107**, 177002 (2011); M. Houzet, J. S. Meyer, D. M. Badiane, and L. I. Glazman, *Phys. Rev. Lett.* **111**, 046401 (2013).
- [34] I. Garate and K. Le Hur, *Phys. Rev. B* **85**, 195465 (2012).
- [35] R. Ilan, J. Cayssol, J. H. Bardarson, and J. E. Moore, *Phys. Rev. Lett.* **109**, 216602 (2012).
- [36] C. W. J. Beenakker, D. I. Pikulin, T. Hyart, H. Schomerus, and J. P. Dahlhaus, *Phys. Rev. Lett.* **110**, 017003 (2013).
- [37] G. Barak, H. Steinberg, L. N. Pfeiffer, K. W. West, L. I. Glazman, F. von Oppen, and A. Yakoby, *Nature Phys.* **6**, 489 (2010).
- [38] T. Karzig, L. I. Glazman, and F. von Oppen, *Phys. Rev. Lett.* **105**, 226407 (2010).
- [39] D. M. Gangardt and A. Kamenev, *Phys. Rev. Lett.* **104**, 190402 (2010).
- [40] T. Micklitz and A. Levchenko, *Phys. Rev. Lett.* **106**, 196402 (2011).
- [41] K. A. Matveev and A. V. Andreev, *Phys. Rev. B* **86**, 045136 (2012).
- [42] A. Lamacraft, *Phys. Rev. A* **87**, 012707 (2013).
- [43] M. Octavio, M. Tinkham, G. E. Blonder, and T. M. Klapwijk, *Phys. Rev. B* **27**, 6739 (1983).
- [44] K. E. Nagaev, *Phys. Rev. Lett.* **86**, 3112 (2001).